

This is a repository copy of *Evidence of high-n hollow-ion emission from Si ions pumped by ultraintense x-rays from relativistic laser plasma.*

White Rose Research Online URL for this paper:

<https://eprints.whiterose.ac.uk/103725/>

Version: Accepted Version

---

**Article:**

Colgan, J., Faenov, A. Ya, Pikuz, S. A. et al. (17 more authors) (2016) Evidence of high-n hollow-ion emission from Si ions pumped by ultraintense x-rays from relativistic laser plasma. EPL. 35001. ISSN 1286-4854

<https://doi.org/10.1209/0295-5075/114/35001>

---

**Reuse**

Items deposited in White Rose Research Online are protected by copyright, with all rights reserved unless indicated otherwise. They may be downloaded and/or printed for private study, or other acts as permitted by national copyright laws. The publisher or other rights holders may allow further reproduction and re-use of the full text version. This is indicated by the licence information on the White Rose Research Online record for the item.

**Takedown**

If you consider content in White Rose Research Online to be in breach of UK law, please notify us by emailing [eprints@whiterose.ac.uk](mailto:eprints@whiterose.ac.uk) including the URL of the record and the reason for the withdrawal request.

---

# Evidence of high- $n$ hollow ion emission from Si ions pumped by ultraintense x-rays from relativistic laser plasma

J. COLGAN<sup>1</sup>, A. YA. FAENOV<sup>2,3</sup>, S. A. PIKUZ<sup>3,4</sup>, E. TUBMAN<sup>5</sup>, N. M. H. BUTLER<sup>6</sup>,  
J. ABDALLAH, JR.<sup>1</sup>, R. J. DANCE<sup>6</sup>, T. A. PIKUZ<sup>3,7</sup>, I. YU. SKOBELEV<sup>3,4</sup>,  
M. A. ALKHIMOVA<sup>3,4</sup>, N. BOOTH<sup>8</sup>, J. GREEN<sup>8</sup>, C. GREGORY<sup>8</sup>, A. ANDREEV<sup>9,10</sup>,  
R. LÖTZSCH<sup>11</sup>, I. USCHMANN<sup>11</sup>, A. ZHIDKOV<sup>7</sup>, R. KODAMA<sup>2,7</sup>, P. MCKENNA<sup>6</sup>, AND  
N. WOOLSEY<sup>5</sup>

<sup>1</sup> *Theoretical Division, Los Alamos National Laboratory, Los Alamos, NM 87545, USA*

<sup>2</sup> *Institute for Academic Initiatives, Osaka University, Suita, Osaka 565-0871, Japan,*

<sup>3</sup> *Joint Institute for High Temperatures, Russian Academy of Sciences, Moscow 125412, Russia*

<sup>4</sup> *National Research Nuclear University MEPhI, Moscow, 115409, Russia*

<sup>5</sup> *York Plasma Institute, Department of Physics, University of York, York YO10 5DD, United Kingdom*

<sup>6</sup> *SUPA, Department of Physics, University of Strathclyde, Glasgow G4 0NG, United Kingdom*

<sup>7</sup> *PPC Osaka University and JST, CREST, 2-1, Yamadaoka, Suita, Osaka 565-0871, Japan*

<sup>8</sup> *Central Laser Facility, STFC Rutherford Appleton Laboratory, Didcot, Oxfordshire OX11 0QX, United Kingdom*

<sup>9</sup> *Max Born Institute, Berlin 12489, Max-Born str. 2a, Berlin, Germany*

<sup>10</sup> *ELI-ALPS, Szeged H-6720, Hungary*

<sup>11</sup> *Institut für Optik und Quantenelektronik, Friedrich-Schiller-Universität Jena, Max-Wien Platz 1, D-07743 Jena, Germany*

PACS 52.20.Hv – First pacs description

**Abstract** – We report on the first observation of high- $n$  hollow ions (ions having no electrons in the K or L shells) produced in Si targets via pumping by ultra-intense x-ray radiation produced in intense laser-plasma interactions reaching the radiation dominant kinetics regime (RDKR). The existence of these new types of hollow ions in high energy density plasma has been found via observation of highly-resolved x-ray emission spectra of silicon plasma. This has been confirmed by plasma kinetics calculations, underscoring the ability of powerful radiation sources to fully strip electrons from the inner-most shells of light atoms. Hollow ions spectral diagnostics provide a unique opportunity to characterize powerful x-ray radiation of laboratory and astrophysical plasmas. With the use of this technique we provide evidence for the existence of the RDKR via observation of asymmetry in the observed radiation of hollow ions from the front and rear sides of the target.

---

The ability of bright photon sources to rapidly remove the inner-shell electrons from atoms has become an exciting area of research in recent years since it encompasses a region that lies on the boundary of atomic and plasma physics. This is in part due to the increas-

40 ing availability of such radiation-generating sources as XFELs [1–5] and next-generation  
41 petawatt laser facilities that can generate high-intensity x-ray fields [6]. These experimen-  
42 tal platforms have been used to create novel states of matter with empty inner sub-shells  
43 [2–11], explore the phenomena of continuum lowering [12] and of saturable absorption [13],  
44 and to explore the regime where the radiation interaction dominates the plasma kinetics  
45 [16]. Such investigations, as well as complementary simulations (for example, [14, 15]) help  
46 our understanding of high energy density plasmas of importance in astrophysics [17–19],  
47 inertial confinement fusion [20], and the bright x-ray sources are also of use in biological  
48 imaging and in materials science [21]. Recent reviews [10, 11, 22] have explored in detail the  
49 mechanisms of hollow ion emission in a variety of experimental contexts.

50 The term ‘hollow ion’ has had a number of definitions over the years [23, 24] but is  
51 generally taken to mean atomic states in which the  $K$  shell (and sometimes  $L$  shell) is  
52 partly or fully stripped. Recent measurements on the petawatt scale on thin Al targets  
53 [7] indicated the formation of ions with empty  $K$ -shells, identified by x-ray emission from  
54 the transition of a  $2p$  electron into the  $1s$  subshell. Indeed, all reported observations of  
55 hollow ions have used the same  $2p \rightarrow 1s$  transition to identify such states (whether single-  
56 or double-core hole states). Due to the small likelihood of a double  $K$ -shell ionization, a  
57 detectable  $KK$  hollow ion  $2p-1s$  transition requires a strong driving mechanism. A strong  
58 radiation field [8] has been shown to be much more efficient at ionizing the  $K$ -shell compared  
59 to, say, collisions with hot electrons.

60 In this Letter, we demonstrate for the first time that hollow ions can be identified that  
61 have no electrons in both the  $K$  or  $L$  shells, labeling such states ‘high- $n$  hollow ions’. Such  
62 states in Si are identified by the emission of photons corresponding to the  $3p \rightarrow 1s$  transition  
63 that occurs in a lower wavelength range, between the  $Ly_\beta$  and  $He_\beta$  line positions, compared  
64 to the previously-observed hollow ion emission that occurs between the  $Ly_\alpha$  and  $He_\alpha$  line  
65 positions. A diagram of observed transitions in Si that are discussed in this paper is presented  
66 in Fig. 1. The hollow ion emission characterized by  $2p \rightarrow 1s$  transitions in moderately ionized  
67 ions occurs around 6.4 Å (for double-core hole states) and around 6.9 Å (for single-core  
68 hole states). High- $n$  hollow ion emission occurs around 5.4 Å, i.e. between the  $Ly_\beta$  (at  
69 5.2 Å) and  $He_\beta$  (at 5.68 Å) line positions.

70 A schematic of the experimental set-up and a diagram of hollow ion formation and  
71 detection in our experiments are shown in Fig. 2. The measurements were made at the  
72 Vulcan Petawatt laser facility at the Rutherford Appleton Laboratory [25], which generates  
73 a beam using OPCPA technology with a central wavelength of 1054 nm and FWHM duration  
74  $\sim 0.5$ –1 ps. In this experiment approximately 114 J was delivered to the target surface by  
75 a p-polarized laser pulse, focused by an  $f/3$  off-axis parabola at an incident angle of  $45^\circ$   
76 from its surface normal. The energy was contained in a focal spot with diameter of 7  $\mu\text{m}$ ,  
77 resulting in an intensity of  $3 \times 10^{20}$  W/cm<sup>2</sup> on the target, which comprised 2  $\mu\text{m}$  Si wafers,  
78 sandwiched between two 1.6  $\mu\text{m}$  CH layers. **The contrast of the laser was  $10^{-10}$ , which  
79 was important in identifying and interpreting the hollow atom emission. The high contrast  
80 ensured minimal prepulse effects so that the main pulse interacted with an undisturbed,  
81 cold target.** Four Focusing Spectrometers with Spatial Resolution (FSSR) [26] captured  
82 the resultant emission, with two positioned in front of the target and two behind, with two  
83 wavelength ranges covered as indicated in Fig. 3. Image plate detectors covered by different  
84 filters were used for the diagnosis of spectra from all spectrometers, with the exception of  
85 the Front 1 spectrometer in which a back-illuminated CCD was used. Strong magnets were  
86 placed in front of the spectrometers in order to reduce background x-ray noise generated by  
87 fast electrons. The spectrometers were cross-calibrated so that their intensities are directly  
88 comparable.

89 We observe experimentally that the emission recorded on the front spectrometers is in  
90 general more intense than that of the rear spectrometers. However, we find that the ratio  
91 of the  $Ly_\alpha$  to  $He_\alpha$  lines (at 6.18 Å and 6.65 Å respectively) is larger from the Rear 2  
92 spectrometer than from the Front 2 spectrometer. At first this seems to imply that the bulk

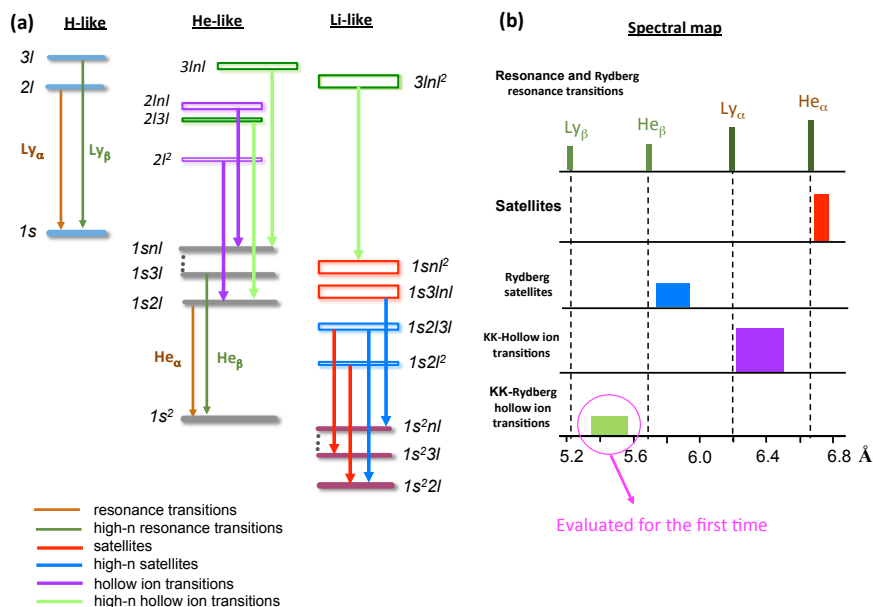


Fig. 1: Schematic diagram of the hollow ion and high- $n$  hollow ion line positions in H-like through Li-like Si ions: (a) the type of transition; (b) the wavelength positions. The resonance and satellite transitions have one electron in the  $K$ -shell in the upper levels, whereas hollow ion and high- $n$  hollow ion transitions have no  $K$ -shell electrons in the upper levels. Furthermore, the high- $n$  hollow ions have no electrons in the  $L$ -shell in the upper levels.

plasma temperature is hotter on the rear surface than on the front surface, which is at odds 93  
 with the lower intensity recorded on the rear spectrometers compared to the front. However, 94  
 we find that emission is also observed between the Ly $\alpha$  and He $\alpha$  lines. Such emission arises 95  
 from KK hollow ion transitions [7] and implies that hollow ion emission is contributing 96  
 strongly to the spectrum measured by the Rear 2 spectrometer. We have performed plasma 97  
 kinetics modeling calculations for Si using the Los Alamos suite of atomic physics codes 98  
 (for an overview, see [27]) to help understand these measurements. Atomic structure and 99  
 collision calculations were performed [28–30] and the ATOMIC code [31–33] was used to 100  
 produce emission spectra for a variety of plasma temperatures and densities. 101

The modeling of the complex emission spectra measured from this plasma is difficult 102  
 due to the spatially and temporally integrated nature of the recorded spectra. In principle, 103  
 hydrodynamic simulations could be used to predict the density and temperature profile of 104  
 the plasma as a function of space and time - but unfortunately such simulations are quite 105  
 difficult to perform and also require various assumptions concerning laser energy absorption, 106  
 material properties, etc. However, we have found from experience [7] that the complex 107

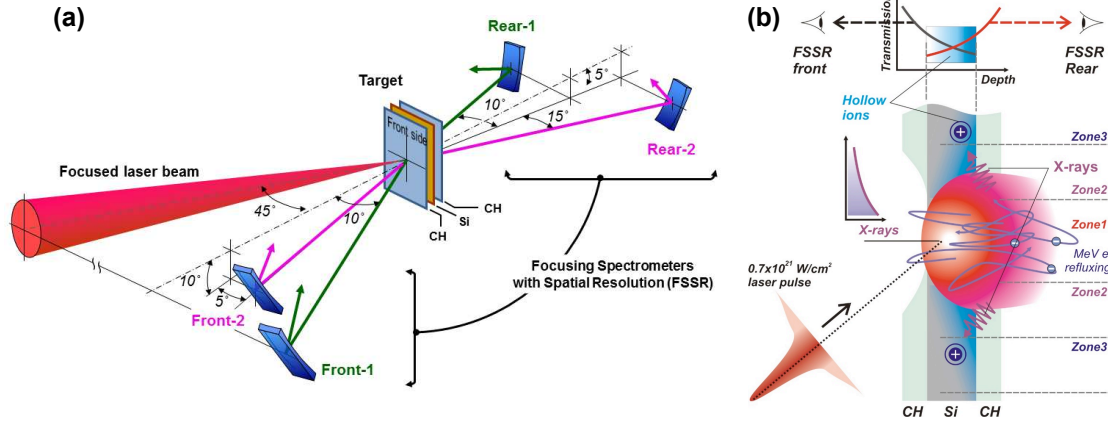


Fig. 2: (a) Experimental design. (b): A schematic diagram of hollow ion formation by the ultra-intense optical laser pulse and its detection from both sides of the target. A laser field in the central area of the focal spot of the target accelerates multi-MeV electrons along the laser beam propagation. Refluxing electrons generate bright x-ray radiation with photons of  $\sim$ keV energies, which creates hollow ions in the outer area of the focal spot. X-ray spectra of hollow ions, emitted by the plasma periphery and measured by FSSR spectrometers from the front and rear sides of target, have different intensities due to differences in absorption of x-ray radiation, which reach the front and rear sides spectrometers. The stronger x-ray pump intensity of the rear side compared with the front side target surfaces is due to target bending from laser radiation pressure from the relativistic laser beam.

108 emission spectra can be reasonably modeled by ATOMIC calculations that assume that the  
 109 plasma is (arbitrarily) divided into just a few zones at particular temperatures and densities.  
 110 This allows some insight into the conditions that may exist within the plasma, as well as  
 111 allowing an understanding of what emission features arise from plasma at a particular set  
 112 of conditions.

113 In this case, we find that the measured emission spectra can be reasonably reproduced  
 114 by 3 plasma zones, as indicated in fig. 2b. The first, central, zone contains bulk plasma  
 115 at high electron temperatures ( $kT_e$ ) of 400 eV (for the rear side of the target) or 550 eV  
 116 (front side) and an electron density ( $N_e$ ) of  $10^{22} \text{ cm}^{-3}$ . This is the region that has directly  
 117 absorbed most of the laser energy, and as a result, is highly ionized.

The second plasma zone surrounds the central zone and is postulated to be at a lower electron temperature of 180 eV and an  $N_e$  of  $3 \times 10^{23} \text{ cm}^{-3}$  (close to solid density conditions). This zone feels a radiation field at a temperature of 2 keV, which arises from the radiation (mostly Bremsstrahlung) emitted from the high energy refluxing electrons formed in the focus of the laser spot. The third plasma zone lies beyond the second plasma zone, and is thought to be at a cooler temperature of 10 eV, again with an  $N_e$  of  $3 \times 10^{23} \text{ cm}^{-3}$ . This zone feels a radiation field at 3 keV. We also postulate that a portion of this zone may also see an enhanced (by a factor of 5) radiation field, the reason for which is discussed in detail in the following paragraphs. All our ATOMIC calculations include continuum lowering [34], a 1% hot electron component, and self-absorption effects via escape factors assuming a  $6 \mu\text{m}$  thickness. The theoretical modeling calculations show that, while a bulk plasma at **zone 1** conditions provides a reasonable match to the  $\text{Ly}_\alpha$  and  $\text{He}_\alpha$  lines (as well as their satellites), we require additional emission from the other plasma zones (see fig. 2b) to match the observed spectrum. Because of the time-integrated nature of the measured spectrum we had to make assumptions about the duration time of the emission from the zones. Generally, the emission from zones 2 and 3 was assumed to be of much shorter duration than the emission from zone 1. An ATOMIC calculation at zone 2 conditions produces significant emission around 6.2 Å, enhancing the emission at exactly the  $\text{Ly}_\alpha$  wavelength. Addition of another ATOMIC calculation at similar conditions but with a smaller  $kT_e$  of 90 eV also improves the comparison with the measured spectrum. Thus, without consideration of emission from hollow ions, **that are only prominent when a strong radiation field is included in the modeling**, one would estimate a hotter temperature in this plasma than may actually exist.

Further evidence for the existence of hollow ion emission is found from ATOMIC calculations at **zone 3 conditions** which provides neutral K-shell emission lines around 7.1 Å (as well as weaker lines around 6.5 Å). If we postulate that the radiation field produced by the refluxing electrons may be enhanced in some spatial regions (by a factor of 5 in this case), as discussed in detail recently [16], we find that such ATOMIC calculations predict weak emission around 6.4 Å, in good agreement with the measured spectrum. This indicates that the plasma conditions under investigation may be entering the radiation-dominated kinetic regime (RDKR) as also found in ultra-intense laser measurements performed recently [7–9, 16].

Returning to the spectrum recorded on the Front 2 spectrometer (Fig. 3b), we find that it is quite well matched by an ATOMIC calculation at zone 1 conditions of  $kT_e$  of 550 eV and  $N_e$  of  $10^{22} \text{ cm}^{-3}$ , and that the contributions from plasma zones 2 and 3 under the influence of the x-ray field are much smaller. This suggests that hollow ion emission is only observed (in the longer wavelength region) from the rear of the target as shown in Fig. 3d. We also note that the  $\text{He}_\alpha$  line and its satellite features are shifted in the measurement compared to the calculation by about 0.02 Å. This is due to fast ion motion of the He-like ions, which corresponds to a ion motion speed of approximately  $10^8 \text{ cm/s}$  with ion energy of  $\sim 150 \text{ keV}$ . Such an effect has previously been observed [35].

The spectra recorded by the Front 1 and Rear 1 spectrometers (left panels of Fig. 3) cover the wavelength range of Si that includes emission from the  $\text{Ly}_\beta$  (5.22 Å),  $\text{Ly}_\gamma$  (4.95 Å), and  $\text{He}_\gamma$  (5.41 Å) lines. While these lines are reasonably prominent in the measured data, we also find significant emission between these lines. ATOMIC calculations from bulk plasma at nominal conditions of electron temperature ( $kT_e$ ) of 400 eV (rear spectrometer) or 550 eV (front spectrometer) and electron density ( $N_e$ ) of  $10^{22} \text{ cm}^{-3}$  provide a good match to the He-like and H-like features, but do not produce emission in the regions between these lines. However, ATOMIC calculations at lower electron temperatures (90 eV), which were also used to explain the hollow ion spectra formation from the Front 2 and Rear 2 spectrometers, and that include a x-ray radiation field (at 2 keV), *do* provide such emission and also improve the agreement with the measured emission around 5.0 Å. The transitions that are prominent from such calculations arise from what we term *high-n hollow ions*, that is, transitions from

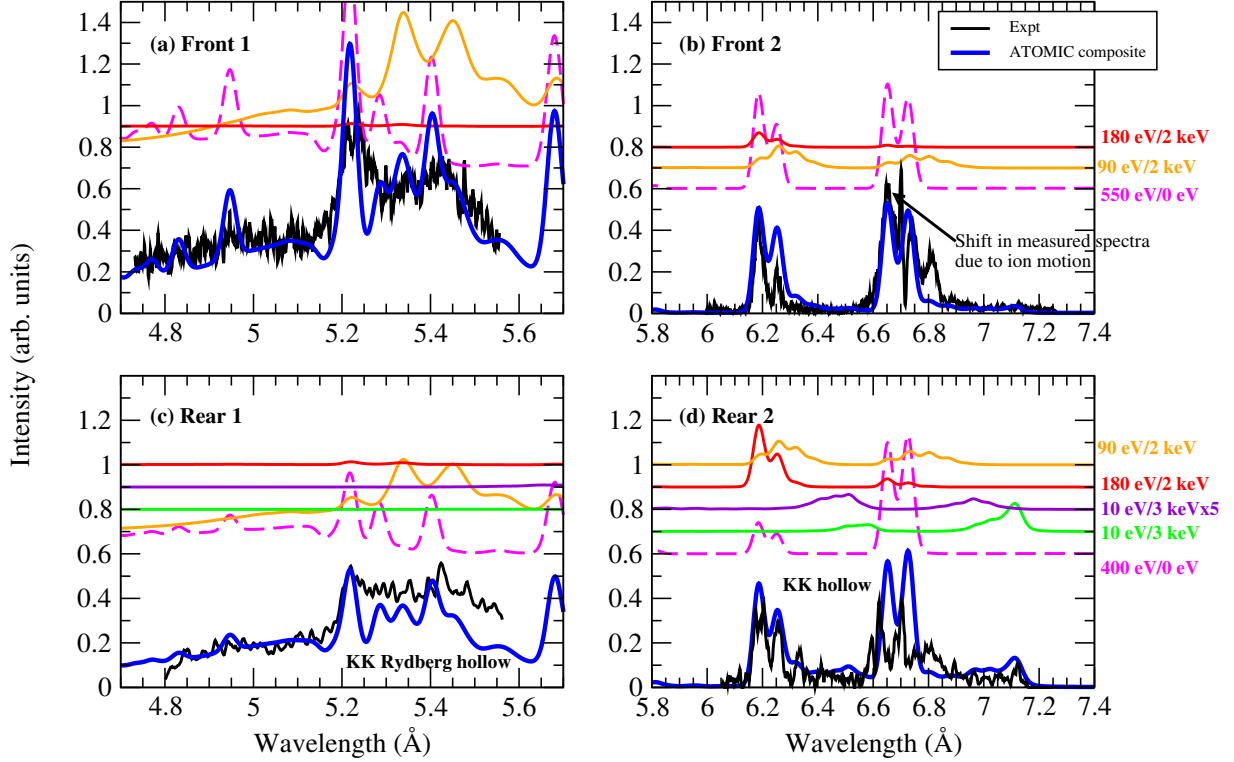


Fig. 3: Comparison of measured spectra from the four spectrometers shown in Fig. 2 and composite ATOMIC calculations as indicated, assuming emission from various plasma zones (see fig. 2b). The experimental spectra are presented with a common calibration so that the intensities in each panel are comparable. The thick blue lines represent the composite ATOMIC calculations that are the sum of calculations at specific temperatures and densities as follows. The ATOMIC calculations are performed for a bulk electron temperature ( $kT_e$ ) of 550 eV for the front spectrometers and a  $kT_e$  of 400 eV for the rear spectrometers, for an electron density ( $N_e$ ) of  $10^{22} \text{ cm}^{-3}$  (for zone 1). We include contributions from calculations at  $kT_e=180 \text{ eV}$  and  $kT_e=90 \text{ eV}$ , both using a radiation field ( $kT_r$ ) of 2 keV and  $N_e=3 \times 10^{23} \text{ cm}^{-3}$  (for zone 2). The comparisons of the spectra from the rear spectrometers also include a calculation at  $kT_e=10 \text{ eV}$ ,  $kT_r=3 \text{ keV}$ , as well as a calculation at  $kT_e=10 \text{ eV}$ , with a  $kT_r=3 \text{ keV}$  that is enhanced by a factor of 5 (all at  $N_e=3 \times 10^{23} \text{ cm}^{-3}$ ) (for zone 3). The individual ATOMIC calculations are offset for clarity.

171 the  $3p$  subshell to the empty  $1s$  ( $K$ ) shell of Li-like (and other) Si ions. We are unaware  
 172 of any previous observations of such transitions, although a previous study [36] postulated  
 173 the existence of such transitions in quasi-continuous spectra. **These high- $n$  hollow ions lie**  
 174 **near the  $Ly_\beta$  lines and are of similar intensity. Thus, it is important to consider such states**  
 175 **when analyzing the role of ionization potential lowering in dense plasmas.**

176 To further illustrate the important role played by the x-ray radiation, in Figs. 4 we present  
 177 ATOMIC calculations at an electron temperature of 90 eV made without the radiation  
 178 field for various fractions of hot electrons (at a temperature of 10 keV). We find that even

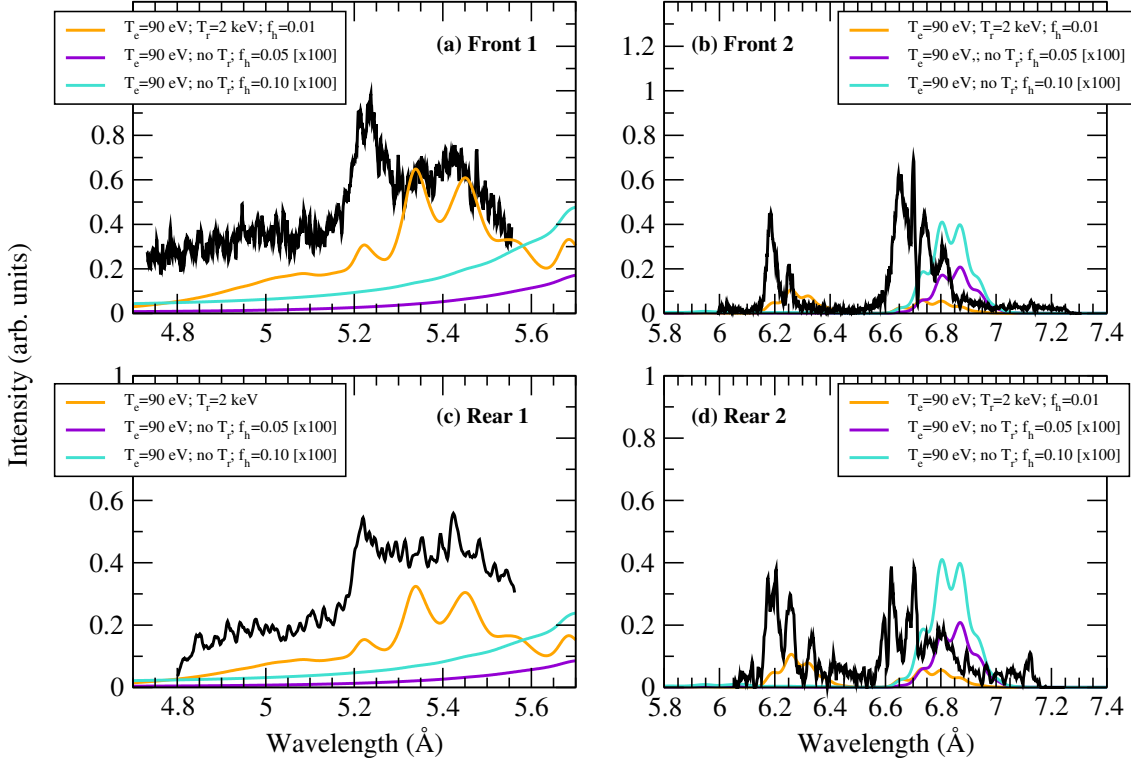


Fig. 4: Comparisons of the measured spectra and ATOMIC calculations at  $kT_e=90$  eV (all at  $N_e=3 \times 10^{23}$  cm $^{-3}$ ). The orange lines show calculations using  $kT_r=2$  keV and 1% hot electrons. The purple and blue lines show calculations using no radiation field, but with 5% and 10% hot electron fraction respectively. Note that the latter two calculations are multiplied by 100 for better visual comparison.

somewhat large hot electron fractions of 10% or more (see Fig. 5) do not produce KK transitions, especially in the region around 6.4 Å, and between 5.2 and 5.4 Å. Similar findings are reached for test calculations at an electron temperature of 10 eV or 180 eV - no KK transitions are observed with hot electrons only. We also note that the intensity of emission from the ATOMIC calculations with only hot electrons is one or more orders of magnitude smaller than the emission found when a x-ray radiation field is used in the calculations. Such calculations support our assertion [8] that an intense x-ray radiation field, produced by the refluxing electrons through the thin target, is the most plausible mechanism for production of the KK hollow ion and high- $n$  hollow ion emission that is found experimentally.

The finding that hollow ion emission is mostly observed from the rear side of the target provides further confidence that the hollow ions are driven by ultra-intense x-ray radiation emission by plasma approaching the RDKR. Indeed, the x-ray pumping source was found to be situated behind the primary, laser-facing, CH foil, curved inward during interaction with the incident laser pulse (and pre-pulse). The absorption of this radiation becomes important due to its role in producing the radiation field. The experimentally observed

194 Doppler shifts of spectral lines confirm the movement of the critical surface toward the  
 195 x-ray source. The mean free path of x-rays can be easily estimated using the Kramers  
 196 approximation for photoionization cross-section as  $l^{-1} = 8 \times 10^{-18} N_Z (I_Z/\hbar\omega)^3 / Z^2 \text{ cm}^{-1}$   
 197 where  $I_Z$  is the ionization potential,  $N_Z$  the ion density,  $Z$  the ion charge, and  $\hbar\omega$  the x-ray  
 198 energy. Assuming  $\hbar\omega \approx I_Z$  one finds that for solid density and  $Z = 10$  that  $l \approx 2.5 \mu\text{m}$ . That  
 199 means in a curved target, x-rays interact mainly with the rear surface. This also explains  
 200 the difference in plasma temperatures seen from the front and rear sides of the target.

201 It should also be noted that even simple detection of hollow ion spectra allows an es-  
 202 timation of the intensity of x-rays pumping the plasma. The hollow ions are excited from  
 203 autoionizing ionic states by photoionization. To produce a sufficient number of hollow ions  
 204 the photoionization must be the main channel of the autoionizing state decay. It means  
 205 that condition  $(I_X/\hbar\omega)\sigma^{ph} \geq G$  must be satisfied (where  $I_X$  is the x-ray pumping flux,  
 206  $\hbar\omega$  is the energy of the x-ray photon,  $\sigma^{ph}$  is the photoionization cross section and  $G$  is the  
 207 probability of autoionization). An estimate finds that for the Si XIII ion the x-ray radiation  
 208 will produce a sufficient number of hollow ions when  $I_X$  is about  $10^{18} \text{ W/cm}^2$  or higher.

209 Our calculations show that observable features of the hollow ion spectra are sensitive  
 210 to In the last few decades a number of diagnostics have been developed for analysis of  
 211 high-temperature plasma. Such diagnostics allow the measurement of important plasma  
 212 parameters such as plasma density, plasma temperature, and hot electron fraction. However,  
 213 no methods exist for determination of the ultraintense x-ray radiation that can strongly  
 214 perturb the plasma. It seems feasible that observation of high- $n$  hollow ion transitions may  
 215 now be used for this purpose.

\* \* \*

216 We thank the Vulcan technical and target preparation teams at the Central Laser Facility  
 217 for their support during the experiments. The research leading to these results has received  
 218 funding from the Science and Technology Facilities Council, and the Engineering and Phys-  
 219 ical Science Research Council (Grant No. EP/J003832/1) of the United Kingdom. The  
 220 Los Alamos National Laboratory is operated by Los Alamos National Security, LLC for the  
 221 NNSA of the U.S. DOE under Contract No. DE-AC5206NA25396. The work is supported  
 222 by Russian Foundation for Basic Research via grants #15-32-21121 and #14-22-02089.

## 223 REFERENCES

- 224 [1] YOUNG L. *et al.*, *Nature*, **466** (2010) 56.  
 225 [2] VINKO S. M. *et al.*, *Nature*, **482** (2012) 59.  
 226 [3] NAGLER B. *et al.*, *Nature Phys.*, **5** (2009) 693.  
 227 [4] WALDROP M. M., *Nature*, **505** (2014) 604.  
 228 [5] MIMURA H. *et al.*, *Nature Comm.*, **5** (2014) 3539.  
 229 [6] PIKUZ S. A. *et al.*, *Physics-Uspekhi*, **57** (2014) 702.  
 230 [7] COLGAN J. *et al.*, *Phys. Rev. Letts.*, **110** (2013) 125001.  
 231 [8] PIKUZ S. A. *et al.*, *High Energy Density Phys.*, **9** (2013) 560.  
 232 [9] HANSEN S. B. *et al.*, *Phys. of Plasmas*, **21** (2014) 031213.  
 233 [10] SKOBELEV I. YU. *et al.*, *Physics-Uspekhi*, **55** (2012) 47.  
 234 [11] FAENOV A. YA. *et al.*, *Laser Part. Beams*, **33** (2015) 27–39.  
 235 [12] CIRICOSTA O. *et al.*, *Phys. Rev. Letts.*, **109** (2012) 065002.  
 236 [13] RACKSTRAW D. S. *et al.*, *Phys. Rev. Letts.*, **114** (2015) 015003.  
 237 [14] ROSMEJ F. B., *Europhys. Lett.*, **55** (2001) 472.  
 238 [15] ROSMEJ F. B. and LEE R. W., *Europhys. Lett.*, **77** (2007) 24001.  
 239 [16] FAENOV A. YA. *et al.*, *Sci. Reports*, **5** (2015) 13436.  
 240 [17] BEIERSDORFER P. *et al.*, *Ann. Review Astron. & Astrophys.*, **41** (2003) 343.  
 241 [18] BEHAR E., SAKO M. and KAHN S. M., *Ap. J.*, **563** (2001) 497.  
 242 [19] SAVIN D. W. *et al.*, *Rep. Prog. Phys.*, **75** (2012) 036901.

- 
- [20] ATZENI S. and MEYER-TER-VEHN J., *The Physics of Inertial Fusion* (Clarendon Press, Oxford) 2004. 243
- [21] BRENNER C. M. *et al.*, *Plasma Phys. Contr. Fusion*, **58** (2016) 014039. 244
- [22] ROSMEJ F. B. *et al.*, *J. Phys. B*, **48** (2015) 224005 245
- [23] BRIAND J.-P. *et al.*, *Phys. Rev. Letts.*, **65** (1990) 159. 246
- [24] MCPHERSON A. *et al.*, *Nature*, **370** (1994) 631. 247
- [25] DANSON C. N. *et al.*, *Laser and Particle Beams*, **23** (2005) 87. 248
- [26] FAENOV A. YA. *et al.*, *Physica Scripta*, **50** (1994) 333. 249
- [27] FONTES C. J. *et al.*, *J. Phys. B*, **48** (2015) 144014. 250
- [28] COWAN R. D., *The Theory of Atomic Structure and Spectra* (University of California Press, Berkeley) 1981. 251
- [29] ABDALLAH J., CLARK R. E. H. and COWAN R. D., *Los Alamos National Laboratory, Los Alamos Manual No. LA 11436-M-I*, **1988** (. 252
- [30] CLARK R. E. H., ABDALLAH JR J. and MANN J. B., *Ap. J.*, **381** (1991) 597. 253
- [31] MAGEE N. H. *et al.*, *14th Topical Conference on Atomic Processes in Plasmas*, edited by J.S. COHEN, S. MAZEVET, AND D. P. KILCREASE (AIP Conference Proceedings, New York) 2004, p. 168–179. 254
- [32] HAKEL P. *et al.*, *J. Quant. Spectr. Rad. Transfer*, **99** (2006) 265. 255
- [33] MAZEVET S. and ABDALLAH, JR. J., *J. Phys. B*, **39** (2006) 3419. 256
- [34] STEWART J. C. and PYATT, JR. K. D., *Ap. J.*, **144** (1966) 1203. 257
- [35] BELYAEV V. S. *et al.*, *JETP Letters*, **81** (2005) 616. 258
- [36] FAENOV A. *et al.*, *Physica Scripta*, **T80** (1999) 536. 259
- [37] ANDREEV A. A. and PLATONOV K. YU., *Laser and Particle Beams*, **18** (2000) 81. 260
- [38] TERNOV M., *Physics-Uspeski*, **38** (1995) 409. 261